Archives Italiennes de Biologie, 135: 95-109, 1997.

THE ENERGETIC COST OF PHOTORECEPTION IN RETINAL RODS OF MAMMALS

G.C. DEMONTIS, B. LONGONI, C. GARGINI AND L.CERVETTO

Istituto Policattedra di Discipline Biologiche, Università di Pisa, Via Bonanno Pisano 6, I-56126 Pisa, Italy

INTRODUCTION

Retinal rods and cones of mammals are complex structures that perform an impressive number of functions within the tiny volume of a few tens of femptoliters. Highly specialised structures at the outer segment are optimised to transduce into an amplified electrical signal the photons they absorb with remarkable efficiency. The signals generated at the outer segment spread then passively along the inner segment and the cell body and eventually reach the synaptic ending; from there, they either depolarise or hyperpolarise the associated retinal neurones by modulating the rate of transmitter release.

The processes associated with both transduction and synaptic transmission have been extensively investigated and unravelled to include also molecular details (22, 21, 25, 5). This is in contrast with the still baffling knowledge on the functions of the inner segment and cell body. These regions, located, perhaps strategically, in between the transductive and synaptic compartments, must cope with the heavy metabolic and synthetic needs of the visual cell.

The existence of a large cationic current flowing passively in darkness across the surface membrane of photoreceptors (12) requires efficient and expensive mechanisms for transporting ions uphill. Energy is also required for a variety of synthetic processes which include, among others, renewal of the specialised outer segment membranes and the production of synaptic transmitter.

There are reasons to believe that the processes occurring at the inner segment of mammalian rods have a control on both signal transduction and transmission. Rod adaptation has been recently found to be influenced by the partial block of $Na+/K^+$ ATPase (10), which is known to operate in rods at the inner segment (23). A variety of ionic conductances have also been described at the inner segment, where they are thought to play an important role in shaping the waveform of the voltage response to light (11, 1, 3, 27).

The aim of the present study is to analyse some of the processes taking place in the metabolic compartments of the visual cell and to evaluate how they interact with specific sensory functions to maintain photoreception efficient and robust.

METHODS

Experiments were performed on male albino guinea-pigs (*Cavia porcellus*) reared according to Institutional guidelines for animal care. Enucleation was performed on animals sacrificed by a lethal dose of anesthetics (300 mg Kg^{-1} ketamine and 80 mg Kg^{-1} thiopental). Dark adapted retinas (2 h) were isolated and chopped under infrared illumination (λ>900 nm) with the help of an infrared converter.

The preparation was then placed in the experimental chamber (volume 350 ml), mounted on an inverted microscope, and perfused with oxygenated buffered Locke solution, whose composition was in mM: NaCl 145; KCl 3.6; $MgCl_2$ 2.4; $CaCl_2$ 1.2; Hepes 5; Na-Ascorbate 0.05; glucose 10.

The experimental chamber, whose body was made of Perspex, was enclosed in a copper block, housing 4 resistors connected to a voltage source. A small thermistor, inside the experimental chamber, provided the feedback to a 8088 microprocessor based personal computer controlling the output of the voltage source. In this way the temperature in the chamber could be set at any level between room temperature, usually 18°C, and 39°C, the body temperature of guinea-pigs.

Membrane current and light response were recorded by means of suction electrodes from rod outer segments attached to small pieces of retina (4). The recording apparatus and light-stimulation were as previously reported (8, 10).

Membrane current was also measured from inner segments of isolated rods by the whole-cell clamp method (13).

RESULTS

The efficiency by which rods signal light changes rests upon a variety of delicately balanced transformations, which ultimately determine the light-sensitivity and the ability to adjust it as a function of the ambient illumination. Most of these transformations are thermodynamically unfavourable and need to be coupled to processes with negative free-energy changes. It seems therefore reasonable to suppose that the extent by which metabolism affects the sensory functions of the visual cell can be best evaluated by measuring both sensitivity and adaptation.

Temperature dependence of light-adaptation.

The temperature dependence of the dark current has been previously investigated. The value of the Q_{10} was found at around 2, which corresponds to an activation energy of about 15 KCal M^{-1} (24, 2, 20, 8, 26).

The effect of varying temperature on the current response of a rod is illustrated in Figure 1. In A are responses to 20 msec light flashes of increasing intensity obtained at 16.6°C. In B are the responses from the same rod at 36.1°C. The normalised response amplitudes at 16°C (open circles) and 36°C (filled circles), measured 300 and 100 msec after light onset respectively, are plotted in panel C. The continuous lines, interpolating the experimental points, are saturating exponentials of the form:

$$\text{equation 1)} \quad \frac{R(I)}{R\ max} = (1-e^{-K_f \cdot I})$$

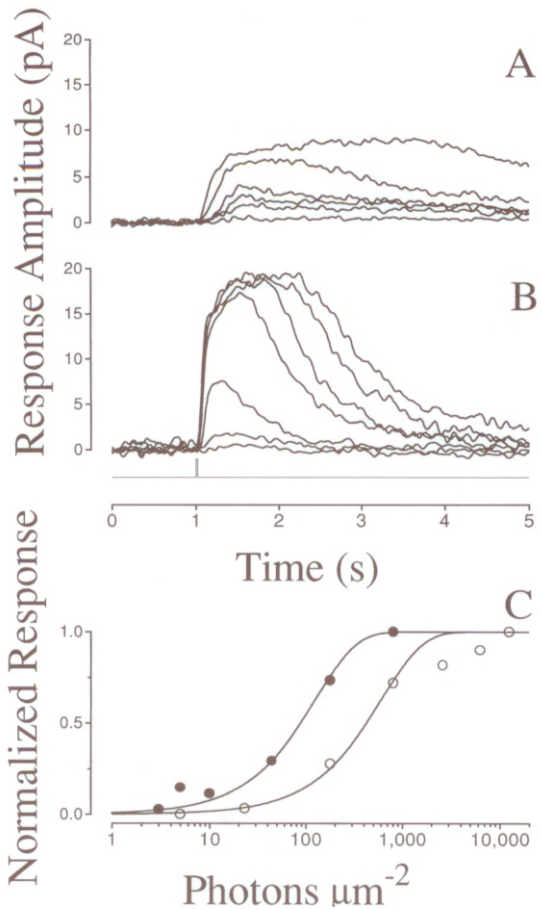

Fig. 1. - *Flash response at two different temperatures.*

Panel A. Responses of a guinea-pig rod to a 20 msecs flash of increasing intensity (3, 5, 10, 44, 179, 813 photons μm^{-2}), measured at 16.6°C. Every trace is the average of 4 sweeps, sampled at 333 Hz, filtered at 20 Hz and digitally smoothed with a 30 msec wide window.
Panel B. Responses, from the same rod as in A (light intensities in photons μm^{-2}: 5, 23, 179, 813, 2643, 6370, 12000), but at 36.1°C. Every trace is the average of 2 sweeps, sampled at 167 Hz, filtered at 30 Hz and digitally smoothed by a 30 msec wide window.
The amplitude of the response, measured 100 msec (open symbols) and 300 msec (filled symbols) after the flash for panel A and B respectively, are plotted normalized in panel C. The continuous lines interpolating the experimental points are best fits to the equation 1, with K_f = 0.0079 (filled circles) and 0.00163 (open symbols) μm^{-2} photon, corresponding to an $I_{0.5}$ of 88 and 425 photons μm^{-2}.

where R(I) is the response amplitude as a function of the light intensity *I*, R_{max} is the maximal amplitude of the dark current and K_f is a constant with the dimension of μm^2 $photon^{-1}$. The half-saturating light intensity ($I_{0.5}$), an indicator of light-sensitivity, was obtained from K_f by the relation: $I_{0.5} = \frac{\ln 2}{K_f}$. In this example raising the temperature from 16.6°C to 36.1°C increased $I_{0.5}$ from 88 to 425 photons μm^{-2}, which corresponds to a decrease in sensitivity of about 0.7 logunits. In other

three rods the change in sensitivity with temperature was somewhat smaller, with an average difference of 0.39±0.1 log units (mean ± S.E.) in the range between 16 and 35°C.

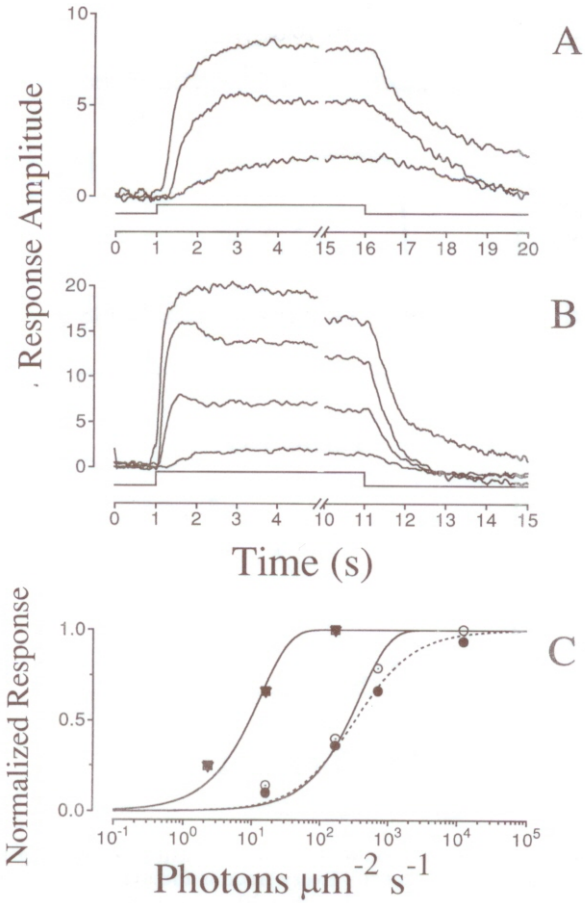

Fig. 2. - *Step response at two different temperatures.*

In A is the response to 15 second steps of light (2, 16 and 171 photons μm^{-2} s^{-1}), from the same rod as in figure 1 at 16.6°C. The stimulation protocol is reported at the bottom of panel A. Note the 5 seconds gap in the time axis. Traces are the average of 4 sweeps, recorded at sampling rate of 6 msec, filtered at 20 Hz and digitally smoothed by a 60 msec time window.
In B are the responses, from the same rod as in A but at 36.1°C, to 10 secs steps of light (16, 171, 715, 12544 photons μm^{-2} s^{-1}), at 36.1°C. A 5 s gap, between 5 and 10 s from background onset, is indicated on the time axis. The traces are the average of 2 sweeps, recorded at a sampling rate of 6 msec, filtered at 20 Hz and digitally smoothed by a 60 msec window.
The normalized amplitudes, measured at peak (open symbols) and 5 s after background onset (filled symbols), are shown in panel C for the traces of panel A (triangles) and B (circles). The continuous lines interpolating the experimental points at peak are saturating exponentials, according to equation 2, with Ks = 0.0745 μm^{-2} $photon^{-1}$ s^{-1} (16.6°C) and Ks = 0.00258 μm^{-2} $photon^{-1}$ s^{-1} (36.1°C). The dashed curve interpolating the normalized response amplitudes mesured 5 s after background onset at 36.1°C is the best fitting hyperbolic relation of the form: $R(I) = \frac{I}{I + 10.5}$, where R(*I*) is the normalised response amplitude as function of I, the background intensity and $I_{0.5}$ is the background intensity giving an half-maximal response. For this cell $I_{0.5}$ was 325 photons μm^{-2} s^{-1}.

Raising the temperature, from 16°C to 36°C, affects both amplitude and kinetics of the photoresponse, as shown in Fig. 1. At 36°C the dark-current amplitude is 19.2 pA, more than two times the value of 8.2 pA measured at 16°C. The activation energy (Ea), obtained from the Arrhenius plot is 11 KCal M^{-1} for this cell and ranged from 10 to 17 in other three rods, with an average value of 12 KCal M^{-1}. The kinetics is accelerated by increasing temperature, as shown by measuring the time to peak which is 100 msec at 36.1°C and 300 msec at 16.6°C.

Changes in sensitivity in rods are usually associated with modifications of the light-adapting properties of photoreceptors. Light-adaptation is recognised by a light-dependent decrease in sensitivity and by the current re-activation during prolonged illumination.

The effect of temperature on current re-activation during steady illumination is illustrated in Figure 2. In A are the responses to steps of light of increasing intensity measured at 16.6°C. At this temperature the kinetics of the photoresponse is slow and sustained. Responses to steady light at 36.1°C are shown for comparison in panel B. In these conditions, at intermediate levels of illumination the response consists of an initial peak, followed by a relaxation which reaches the plateau in 2-3 seconds after the onset of the background illumination.

In panel C the normalized response amplitude, measured at peak (open symbols), or 5 seconds after the onset of steady light (filled symbols), is plotted as a function of the level of illumination. The curve drawn through the experimental points was obtained from a saturating exponential of the form:

$$\text{equation 2)} \quad \frac{R(I)}{R_{max}} = (1 - e)^{-K_S \bullet I}$$

where R(I) is the response amplitude in pA, R_{max} is the dark current amplitude in pA, I is the background intensity in photons μm^{-2} $sec^{-1}$and K_s is a constant.

At 36.1°C (circles), the saturating exponential provides a good fit to the intensity-response curves for measurements taken at the peak. When plateau values are considered, then a better fit is obtained with a hyperbolic relation of the form: $\frac{R(I)}{R_{max}} = \frac{I}{I + EC_{50}}$, where R(I) is the response amplitude, R_{max} is the dark current, I is the background intensity in photons μm^{-2} sec^{-1}, and EC_{50} is the background intensity that induces 50% of the response.

The effect of cooling is reminiscent of that induced by strophanthidin (10), a drug known to selectively inhibit the Na^+/K^+-ATPase. The increase in internal sodium concentration ($[Na]_i$), caused by the pump inhibition, reduces the affinity of the Na^+:Ca^{2+};K^+ exchanger for internal free calcium ($[Ca]_i$) and slows calcium extrusion (10).

The results illustrated in Figure 3 support the idea that also the changes in sensitivity, observed at different temperatures, are associated with differences in the kinetics of calcium extrusion by the exchanger. The light-insensitive component of membrane current (29) attributed to the operation of the exchanger is shown to relax toward zero during the response to a bright flash of light at 16.6°C (A) and 36.1°C (B). The exchange current is normalized to the dark current of 8.2

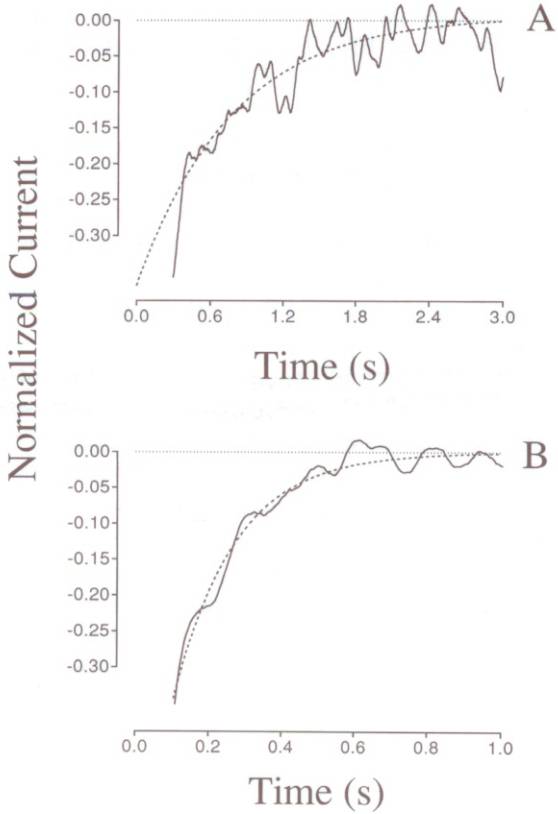

Fig. 3. - *Exchange current at two different temperatures.*

Light-insensitive components of the membrane current measured after a bright, 20 msec, flash delivering 813 photons μm^{-2}, from a guinea-pig rod at 16.2°C (A) and 36.1°C (B). The dashed curve in A is the best fit to the experimental data of a single exponential decay process with a time constant, τ = 766 msec. The dark current was 8.2 pA.
The dashed curve in B is the best fit to data of a monoexponential decay process with τ = 168 msec. The dark current was 19.2 pA. The zero current level is indicated by the dotted line in both panels. The traces are the average of 4 and 2 sweeps for panel A and B respectively. Sampling rate was 3 ms for panel A and 6 msec for panel B. Data were filtered at 20 Hz and digitally smoothed by a 30 msec. wide window.

(A) and 19.2 pA (B), and fitted (dashed curve) by a single exponential with a time constant of 722 msec (A) and 166 msec (B).

The effect of temperature on sensitivity and adaptation as well as those induced by pump inhibitors may ultimately be explained by a change in $[Na]_i$. A further contribution to $[Na]_i$ turn-over in rods come from the existence of voltage-dependent conductances, located at the rod inner segment. Figure 4 illustrates current measurements obtained in whole-cell voltage-clamp from the inner segment of a guinea-pig rod. Hyperpolarizing and depolarising voltage steps from an holding potential of -40 mV, a value which is close to the rod membrane potential in darkness, activate time and voltage dependent currents as shown in the middle

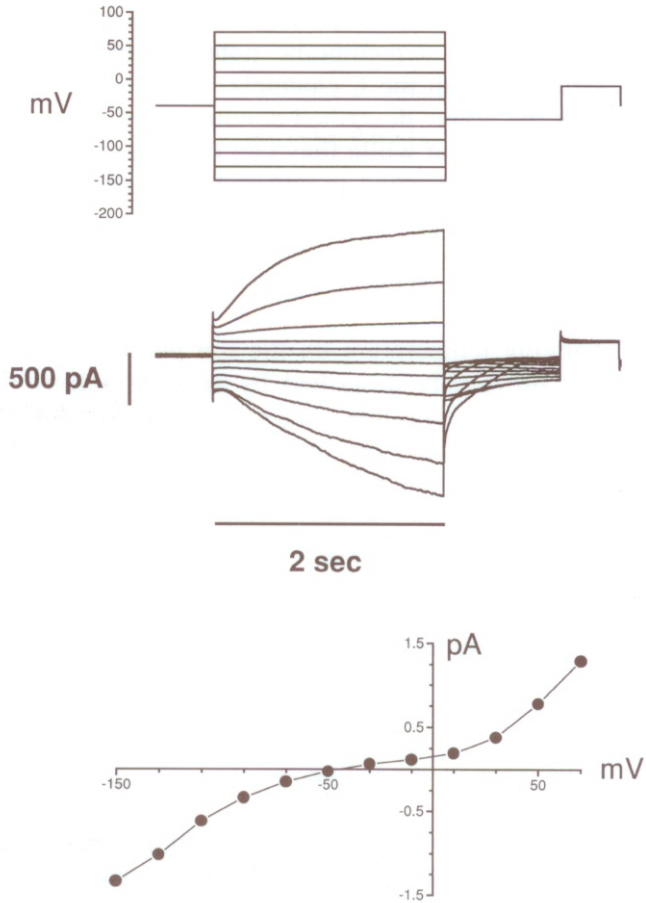

Fig. 4. - *Voltage-dependent currents of guinea-pig inner segment.*

Voltage pulses of 2 s duration were applied, from an holding voltage of -40 mV, to an isolated guinea-pig rod (in the upper panel) and the whole-cell clamp current recorded in these conditions is illustrated in the middle panel. The current amplitudes, measured at the end of the 2 s voltage steps, are plotted as a function of the activating voltage. The traces were sampled at 500 Hz and filtered at 200 Hz by a four pole Bessel filter. The series resistance of 30 MΩ was 50 % compensated.

panel of figure 4. The I/V relation, measured at the end of the 2 second activating voltage steps, is S-shaped, as shown in the bottom panel. Outward rectification is likely to include a substantial Cl- conductance, since on repolarization to -70 mV, close to the potassium reversal potential, a large inward current is observed as expected for a ion whose reversal potential is close to 0 mV. Inward rectification in retinal rods has been previously attributed to I_h, whose activation during the light-response is responsible for the characteristic waveform of the voltage response of both amphibian (11, 3, 1) and mammalian rods (27). The response is characterised by an initial hyperpolarizing peak, quickly sagging to a much depolarised level. A typical feature of I_h is its permeability to both sodium and potas-

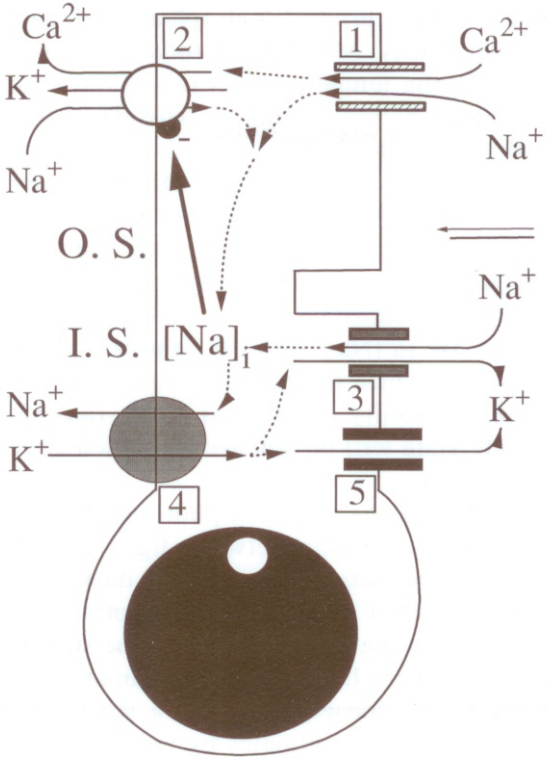

Fig. 5. - *The main mechanisms involved in the regulation of $[Ca]_i$ and $[Na]_i$ as presented in schematic form.*

$[Ca]_i$ turn-over is controlled by the balance between the influx through the light-sensitive channel, indicated by the box 1, and the uphill extrusion through the $4Na^+:1Ca^{2+};1K^+$ exchanger, indicated by the box 2.
$[Na^+]$ turn-over is controlled by the balance between influx and efflux. Influx is through the light-sensitive channel, the exchanger and the hyperpolarization activated channel, indicated by the box 3. Efflux is carried out by the Na^+/K^+ ATPase located at the inner segment and labelled by the box 4. The inner segment channel, labelled by the box 5, is the potassium channel which closes the circuit for the dark current circulating between outer and inner segment.
Note that any change in $[Na]_i$ will affect the exchanger leading to a change in $[Ca]_i$.

leaking out through specific channels located at the inner segment closes the dark current loop (12).

Despite close similarities, between the effects of strophanthidin and those of cooling, it is important to note, however, that the action of Na^+/K^+ pump inhibitors and that of temperature are not identical. The rising phase of the photoresponse, for instance, is not appreciably affected by strophanthidin, but clearly slowed by cooling. These observations suggest that while the pump inhibitor and the associated rise in $[Na]_i$ do not interfere with the activation steps involved in signal transduction (10), temperature must influence the enzymatic steps involved in the transduction cascade.

Another difference between the effects of strophanthidin and those of temperature is their degree of reversibility. Mammalian rods can be kept for hours at 4°C in Locke solution and when the temperature is raised their dark current quickly increases, with a Q10 ranging between 2 and 3. The effect of strophanthidin has been found to be reversible, provided exposures to the drug were short-lasting (10). Prolonged exposure to the inhibitor invariably resulted in irreversible damage of the visual cell. Both cooling and strophanthidin reduce $[Na]_i$ turn-over by inhibiting the Na^+/K^+ pump, but they do it in different ways. Strophanthidin blocks the pump in the E_2~P configuration, thus preventing the modulation of the ATPase activity by $[Na]_i$. Under these circumstances the steady influx of sodium in the dark will cause an uncontrolled rise in $[Na]_i$ until the complete suppression of the dark current. Cooling may instead reduce the rate of translocation at a given $[Na]_i$, but leave the pump with the possibility of increasing the rate of pumping as $[Na]_i$ raises. In this way a steady-state will be reached, in which a residual dark current can still be modulated by light.

As suggested by Hodgkin (16), the design of photoreceptors as dark sensor, may implement a form of metabolic sharing between light and dark. This idea was supported by the estimates of the metabolic cost of the dark current in rat rods (12). Specifically they estimated a rather high ATP consumption in darkness, 2.5×10^{-16} moles rod^{-1} sec^{-1}, mostly used by the pump to balance the steady inflow of positive cations, through the outer segment light-sensitive channels. This early study was the first to note the metabolic consequences of a sustained sodium influx in darkness. We will now extend these estimates by including the contribution of I_h channels and by comparing the energy load of a rod in the dark and during illumination.

The metabolic cost of the dark-current.

The current flowing in darkness across the surface membrane of a rod (J_T) is the sum of a light-sensitive component, due to passive flux trough the cGMP sensitive channels (J_D) and a light-insensitive current (Je_x), associated with the electrogenic operation of the exchanger (29). Sodium flows inwardly through the light-sensitive channels ($J_{Na(D)}$) (6, 15) and is transported in by exchange with Ca^{2+}. Assuming then that most of the J_D is carried by Na^+ and Ca^{2+} and considering that the Ca^{2+} contribution to J_D corresponds to a value of twice J_{Ex} we have:

$$J_{Na\,(D)} = \frac{J_T - 3 \cdot J_{Ex}}{F \cdot V}.$$

Considering then the stoichiometry of the exchanger (7), the fraction of sodium transported ($J_{Na(ex)}$) into the cell will be:

$$J_{Na\,(ex)} = \frac{4 \cdot J_{ex}}{F \cdot V}.$$

Because on average J_{ex} in a rod is about 7% of the total membrane current it turns out that with a J_T of 30 pA, the sodium component will be 14.5 mM sec^{-1}.

The metabolic cost paid by the cell to offset such a massive influx and to maintain $[Na]_i$ at the comfortable level of 10 μM can be obtained considering that the hydrolysis of 1 ATP powers the exchange of 3 sodium ions. The estimated influx of sodium of 14.5 μM sec^{-1} will then require 4.8 μM ATP sec^{-1} to keep $[Na]_i$ at steady-state.

In addition to the energy supplied to the metabolic pump, a rod in darkness must dissipate energy in at least two other sets of processes, such as those associated to the spontaneous isomerization of rhodopsin and to the synthesis of chemical transmitter molecules. In the present paper however we should consider only the spontaneous isomerization of rhodopsin. In general, every rhodopsin molecule, when activated (Rh*) either spontaneously or by light, requires between 2 and 9 ATP molecules for quenching of Rh*. A variable number of transducin molecules (100 - 10,000) is then activated sequentially by a single Rh* and activation of transducin (T*) requires a GTP molecule.

The rate of rhodopsin isomerization in darkness is given by the equation $\frac{dRh\ (t)}{dt} = K \bullet Rh\ (t)$, where Rh(t) is the number of rhodopsin molecules in the outer segment at time t and K is the rate constant for spontaneous isomerization of Rh. We will take K as $5.2x10^{-11}$, from the estimate for monkey rods at body temperature (4). The number of Rh in a guinea-pig outer segment is obtained assuming a concentration of 3 μM in a total volume of 0.046 pl. Therefore a guinea-pig rod will contain $83x10^6$ molecule of rhodopsin, and the rate of spontaneous isomerization will be $4.3x10^{-3}$ Rh^* sec^{-1}, corresponding to 1.4 pM sec^{-1} of ATP, assuming that 9 ATP molecules are required for Rh* quenching.

Before being quenched, by phosphorylation and the consecutive capping by arrestin, Rh* will diffuse in the disk membrane and activate sequentially a large number of transducin molecules. The estimates for the number of T^* activated by a single Rh^*, in mammalian rods, range from about 100 to 10,000, and different estimates may reflect methodological differences (25). In the present estimates we will assume a value of 5,000 transducin molecules formed for isomerized rhodopsin every second. Considering that, in a mammalian rod at body temperature, the single photon response is complete in about 0.5 seconds, then, 2,500 GTP molecules will be taken up by transducin following a spontaneous isomerization. Taking into account a rod volume of 0.046 pl, and assuming that every GTP molecule is formed by exchange of an energy-rich phosphate group between GDP and ATP, we have that the formation of T* during a spontaneous event will cost about 0.4 nM ATP s^{-1}.

The energetic cost associated with the cGMP flux in darkness can be estimated from the Michaelis-Menten relation for basal, unstimulated, guanylate cyclase (GC). With a K_m of 274 μM, a turn-over of 1 sec^{-1} and a concentration of GC in the outer segment of 30 μM, the rate of cGMP production will be 23 μM sec^{-1} (17).

All these estimates suggest that, in darkness, the largest component of the metabolic expense is the uphill extrusion of sodium by the Na^+/K^+ATPase.

The metabolic expense during bright illumination.

In order to evaluate the occurrence of a metabolic sharing, as suggested by Hodgkin (16), the energy dissipated in darkness must be compared with that dissipated during exposure to a bright, saturating, light.

In mammalian rods illumination with a light inducing 5,000 isomerization sec^{-1} will close all the light-sensitive channels (8), thus preventing sodium influx through the channels or, after a delay, through the exchanger. In these conditions energy will be required for the quenching of active rhodopsin, for the GTPase activity of active transducin and for the cGMP flux through the maximally active guanylate cyclase.

A bright light isomerizing 5,000 rhodopsin molecules every second will require 1,6 μM ATP sec^{-1}, assuming that every active rhodopsin requires 9 ATP molecules for quenching.

The metabolic cost associated with GTP hydrolysis by transducin is more difficult to estimate, since the number of active transducin produced by a constant light isomerizing, at steady state, 5,000 rhodopsin molecules is presently unknown. In view of the amplification present in the transduction cascade, however, the figure will lie in between the estimate for rhodopsin quenching and those for cGMP hydrolysis and synthesis.

The hydrolysis rate of fully activated phosphodiesterase has been reported as 0.3 μM sec^{-1} (17). In these conditions guanylate cyclase will be fully activated and cGMP synthesis will be 0.23 μM sec^{-1} (17). Therefore, the metabolic cost for signal transduction will be about 0.6 μM sec-1 of high energy phosphate groups. This amount must be added to the energy required to offset the Na^+ influx through the hyperpolarization activated channels.

The contribution of I_h to $[Na]_i$ turn-over may be estimated from the observation that a light closing all the light-sensitive channels will bring the membrane potential from -40 to -60 mV. The current flowing through the I_h channels can be estimated by considering an equivalent model of the rod membrane, with a leakage conductance in parallel with the light-sensitive conductance in darkness and with the I_h conductance in light. A leakage resistance of 1.6 GΩ with an internal battery of -90 mV and a parallel light-sensitive resistance of 2 GΩ with an internal battery of +20 mV, will give a dark potential of -41 mV and an input resistance of 0.9 GΩ, in agreement with ref. (27). A bright, saturating, background light will transiently bring the membrane potential at around -70 mV, activating the I_h, whose resistance and reversal potential are respectively 1.9 GΩ and -25 mV (9). The current of 18.5 pA through the I_h channels is then estimated, from the Goldman-Hodgkin-Katz equation to be carried for 50% by sodium. This sodium current corresponds to 4.3 mMoles sodium sec^{-1} and to an ATP consumption of 1.4 mMoles sec^{-1}.

Therefore the total energetic expense during bright steady illumination is estimated as 2 mMoles ATP sec^{-1}, a value close to that estimated in darkness. This supports the idea that the metabolic load of a photoreceptor is evenly distributed in light and darkness (16).

ATP and glucose turn-over in mammalian rods.

For an assumed internal ATP concentration of 5 mM, we have an ATP turn-over in darkness of approximately 500 msec, a figure close to the internal sodium turn-over. This estimate does not take into account possible sources of high energy phosphate groups, like the creatine/creatine-P system, which buffers ATP and slows its change.

Glucose consumption can be estimated by considering the ATP yeld of oxidative phosphorylation (36 ATP/glucose) and glycolysis (4 ATP/glucose). A rod with an efficient oxidative metabolism, responsible for 90% of ATP production, will require 0.75 mM Glucose-6P sec^{-1}. Assuming an internal concentration of Glucose-6P of 7.5 mM its turn-over can be estimated to be 10 seconds. In these conditions, 1 minute of glucose deprivation is expected to completely suppress the light response of mammalian rods. Making an allowance of 1-2 minutes for the dead spaces, this is in agreement with the observation that light response is blocked after bathing rods for several minutes in glucose free solutions (Demontis and Cervetto, unpublished).

It is worth of note that glucose-6P turn-over will increase to 2.8 seconds when half of the ATP is produced by glycolysis, suggesting that a concomitant suppression of glucose and oxygen availability will rapidly suppress the ability of the visual cells to respond to light.

The observations and the estimates reported here may have interesting implications when considering conditions in which oxygen and blood supply to the retina are altered. It seems reasonable to suppose that metabolic deficits or changes in retinal or choroidal circulation, such as those occurring in a number of vascular diseases, may be detected at very early stages by simple non-invasive determination of visual adaptation.

SUMMARY

The effects of temperature on rod sensitivity and adaptation are analysed in the general context of the energy requirements of photoreception.

The dependence of adaptation on the $[Na]_i$ turn-over appears to be critical in mammalian rods where the metabolic load is particularly heavy because of both temperature conditions and large Na^+ influx.

Estimates of the energy dissipated by rods in darkness and during bright illumination show that the metabolic load is reasonably well distributed. From this analysis it also results that most of the energy, which a rod dissipates in both darkness and light, is needed to keep $[Na]_i$ and $[Ca]_i$ low.

Acknowledgements. - We would like to acknowledge the contribution of Mr. S. Sabatini, who designed and built the device for controlling the temperature in the experimental chamber. This work was supported by grants from the CNR and the MURST (40%) to L.C.

REFERENCES

1. Bader, C.R., Bertrand, R.D. and Schwartz, E.A. Voltage-activated and calcium-activated currents studied in solitary rod inner segments from the salamander retina. *J. Physiol., Lond.,* **331**: 253-284, 1982.
2. Baylor, D.A., Matthews,G. and Yau, K.W. Temperature effects on the membrane current of retinal rods of the toad. *J. Physiol., Lond.,* **337**: 723-734, 1983.
3. Baylor, D.A., Matthews, G. and Nunn, B.J. Location and function of voltage sensitive conductances in retinal rods of the salamander *Ambystoma tigrinum. J. Physiol., Lond.,* **354**: 203-223, 1984a.
4. Baylor, D.A., Nunn, B.J. and Schnapf, J.L. (). The photocurrent, noise and spectral sensitivity of rods of the monkey Macaca fascicularis. *J. Physiol., Lond.,* **357**: 575-607, 1984b.
5. Breton, M.E., Schueller, A.W., Lamb,T.D. and Pugh, E.N. Jr. Analysis of ERG a-wave amplification and kinetics in terms of the G-protein cascade of phototransduction. *Invest. Ophthalmol. Vis. Sci.,* **35**: 295-309, 1994.
6. Capovilla, M., Cervetto, L., Pasino, E. and Torre V. The sodium current underlying the response of toad rods to light. *J. Physiol., Lond.*, **317**: 223-242, 1981.
7. Cervetto, L., Lagnado, L., Perry, R.J., Robinson, D.W. and Mc Naughton, P.A. Extrusion of calcium from rod outer segments is driven by both sodium and potassium gradients. *Nature,* **337**: 740-743, 1989.
8. Demontis, G.C., Bisti, S. and Cervetto, L. Light sensitivity, adaptation and saturation in mammalian rods. *Progr. Brain Res.,* **95**: 15-24, 1993.
9. Demontis, G.C. and Cervetto, L. Hyperpolarization activated current (I_h) and its modulation in mammalian retinal rods. *Biophys. J.*, **68**: A23, 1995.
10. Demontis, G.C., Ratto, G.M., Bisti, S. and Cervetto, L. Effect of blocking the Na^+/K^+ATPase on Ca^{2+} extrusion and light-adaptation in mammalian retinal rods. *Biophys. J.*, **69**: 439-450, 1995.
11. Fain, G.L., Quandt, F.N., Bastian, B.L. and Gerschenfeld, H.M. Contribution of a caesium sensitive conductance increase to the rod photoreceptors. *Nature,* **272**: 467-469, 1978.
12. Hagins, W.A., Penn, R.D. and Yoshikami, S. Dark current and photocurrent in retinal rods. *Biophys. J.,* **10**: 380-412, 1970.
13. Hamill, O.P., Marty, A., Neher, E., Sackmann, B. and Sigworth, F.J. Improved patch-clamp techniques for high resolution current recording from cells and from cell-free membrane patches. *Pflügers Archiv.,* **391**: 85-100, 1981.
14. Hodgkin, A.L. and Keynes, R.D. Active transport of cations in giant axons from Sepia and Loligo. *J. Physiol., Lond.,* **128**: 28-42, 1955.
15. Hodgkin, A.L., McNaughton, P.A. and Nunn, B.J. The ionic selectivity and calcium dependence of the light-sensitive pathway in toad rods. *J. Physiol., Lond.,* **358**: 447-468, 1985.
16. Hodgkin A.L. Recent work on visual mechanisms. *Proc. R. Soc. Lond. B*, **180**: V-XX, 1972.
17. Kaupp, U.B. and Koch, K.W. Role of cGMP and Ca2+ in vertebrate photoreceptor excitation and adaptation. *Ann. Rev. Physiol.,* **54**: 153-175, 1992.
18. Lagnado, L., Cervetto, L. and McNaughton, P.A. Calcium homeostasis in the outer segments of retinal rods from the tiger salamander. *J. Physiol., Lond.,* **455**: 111-142, 1992.
19. Lagnado, L. and Baylor, D.A. Calcium controls light-triggered formation of catalytically active rhodopsin. *Nature,* **367**: 273-277, 1994.

20. LAMB, T.D. Effects of temperature changes on toad rods photocurrents. *J. Physiol., Lond.*, **346**: 557-578, 1984.
21. LAMB, T.D. and PUGH, E.N. Jr. A quantitative account of the activation steps involved in phototransduction in amphibian photoreceptors. *J. Physiol., Lond.*, **449**: 719-757, 1992.
22. LIEBMAN, P.A., PARKER, K.R. and DRATZ, E.A. The molecular mechanism of visual excitation and its relation to the structure and composition of the rod outer segment. *Annu. Rev. Physiol.*, **49**: 765-791, 1987.
23. MCGRAIL, K.M. and SWEADNER, K.J. Immunofluorescent localization of two different Na,K-ATPases in the rat retina and in identified dissociated retinal cells. *J. Neurosci.*, **6**: 1272-1283, 1986.
24. PENN, R.D. and HAGINS, W.A. Kinetics of the photocurrent in retinal rods. *Biophys. J., 12*: 1073-1094, 1972.
25. PUGH, E.N. Jr. and LAMB, T.D. Amplification and kinetics of the activation steps in phototransduction. *Biochim. Biophys. Acta*, **1141**: 111-149, 1993.
26. ROBINSON, D.W., RATTO, G.M., LAGNADO, L. and MCNAUGHTON, P.A. Temperature dependence of the light response in rat rods. *J. Physiol., Lond.*, **462**: 465-481, 1993.
27. SCHNEEWEIS, D.M. and SCHNAPF, J.L. Photovoltage of rods and cones in the macaque retina. *Science,* **268**: 1053-1056, 1995.
28. TORRE, V. The contribution of the electrogenic sodium-potassium pump to the electrical activity of toad rods. *J.Physiol., Lond.*, **333**: 315-341, 1982
29. YAU, K.W. and NAKATANI, K. Electrogenic Na+:Ca2+ exchange in retinal rod outer segment. *Nature,* 311: 661-663, 1984.